UMT PRESS
Journal of Mathematical Sciences and Informatics
Journal Homepage: https://journal.umt.edu.my/index.php/jmsi
eISSN: 2948-3697
DOI: http://doi.org/10.46754/jmsi.2026.06.008

EMPIRICAL EVALUATION OF SPATIAL DYNAMICS OF SAND RESIDUE ON VARIOUS SHOE SOLE MATERIALS USING HARRIS CORNER STRENGTH FOR FORENSIC FOOTWEAR EXAMINATION

NAJAH KHALISAH MOHD YUSAMI[1], ANWAR A.M.A. SALEM[1,2], FAISAL ARIFFIN@OTHMAN[1] AND LOONG CHUEN LEE[1]*

[1]*Faculty of Health Sciences, Universiti Kebangsaan Malaysia, 43600 Bangi, Selangor, Malaysia.*
[2]*Department of Forensic Sciences, Ministry of Interior, Kuwait City, Kuwait.*

**Corresponding author: lc_lee@ukm.edu.my*

ARTICLE INFO

Article History:
Received: 13 January 2026
Revised: 8 March 2026
Accepted: 9 April 2026
Published: 15 June 2026

Keywords:
Forensic science, footwear impression, image processing, Harris corner.

ABSTRACT

Forensic footwear examinations often consider various types of geo-forensic materials that adhere to and or are retained by the soles of shoes. These particulates could potentially provide valuable insights regarding the movements of victims or suspects. Therefore, understanding the spatial dynamics of materials and the factors affecting the transfer, persistence, and recovery is essential for enhancing the reliability of geo-forensic investigations. This study aims to explore the factors affecting the spatial dynamics of residues on the shoe soles, and to determine the relative importance of different regions of the sole at retaining geo-forensic materials. Three volunteer test subjects of varying Body Mass Index (BMI) ratings were recruited for this study. Each of them walked through a sandy substrate using three types of worn footwear with soles made of rubber, Crosslite, and ethylene-vinyl acetate (EVA) foam. Then, the distribution of the sand particles beneath the soles was subsequently documented using digital photography. The captured images underwent preprocessing procedures including grayscale conversion, resizing, and normalisation. Each treated image was then segmented into 10 equal-sized non-overlapping regions, for detailed analysis using the Harris Corner detector. The total of the Harris corner response values within each region was used as a quantitative representation of residue retention, where higher corner strength values indicated greater accumulation of sand particles total. The findings revealed. that EVA foam had the highest retainability, followed by Crosslite and rubber. Meanwhile, the influence of the BMI statuses on the retainability was pronounced only on the rubber-soled shoes. Furthermore, the areas of the sole covering the metatarsal was found to be the most likely retain sandy particles. Overall, the effect of BMI statuses on the retainability of sandy particles was dependent on the material composition of the shoe sole, while the metatarsal region plays a dominant role in residue persistence. The results of this study add to the expanding pool of knowledge in forensic footwear analysis and lay the groundwork for

the creation of increasingly complex analytical frameworks in accordance with the dynamic nature of residue transfer and retention in real-world investigations.

2020 Mathematics Subject Classification:

Introduction

Forensic footwear examinations are essential for establishing the link between the suspects and specific locations. Various kinds of geo-forensic materials could adhere to and be retained by the soles of a suspects shoes. Therefore, trace evidence obtained from soles of a suspects footwear can potentially outline the movements of a person of interest (POI) [1], including sites visited before, during, and after the alleged offence took place [2]. Hence, an examination of the residue from the soles of a suspects footwear may contribute to the forensic reconstruction of a crime scene, particularly soil and sediment found on footwear, which is a valuable forensic tool studied for establishing a suspect's or victim's whereabouts, mobility, travel history and may help investigators associate an individual suspect or victim with a specific locations [3].

By meticulously analysing how trace materials migrate or are transferred between surfaces and understanding the rate at which they diminish, forensic scientists can gain an insight into the sequence or chronological order of events and build a narrative of those past events [4]. In other words, understanding how long those environmental markers adhere to footwear directly influences the success or failure of a forensic analyses, as detectives must work within the timeframe before these crucial traces are naturally lost or degraded through normal wear and tear or environmental exposure [5]. Hence, understanding the transfer, persistence, and recovery qualities of geo-forensic materials under various conditions is essential to preserving its evidentiary value [2]. However, only a handful of studies have been devoted to the evaluation of the persistence of residues on footwear for forensic or evidentiary purposes.

The spatial distribution and temporal persistence of geo-forensic materials on footwear have been evaluated by Morgan *et al.* [6]. The mixing of sediment and the pressure points on the soles was studied through forensic events that mimicked the conditions at a real crime scene. The research paper found that preservation of soil and sediment varied significantly in different areas of the shoe. Later, the researchers focused on the intricate patterns of silt transfer over time on bottom of the shoes [2]. The findings showed that the largest percentage of particles from earlier places visited were preserved in the arch area of the shoe sole, which experiences the least amount of foot pressure. Although considerable research has been conducted on the initial transfer of sediment to footwear, little is known about how different shoe sole materials affect the persistence of geo-forensic materials on footwear.

Image processing tools have been actively applied to the forensic examination of footwear, particularly for footwear image retrieval purposes [7]. Various automatic shoeprint retrieval methods have been proposed over the years by applying a variety of computer vision algorithms, particularly image processing tools. Typically, feature extraction is used to obtain and catalogue key details of footwear impressions via high-definition images [8]. The steps involved in extracting discriminative features from digital images include detecting or identifying local interest points using an edge detector, which were then encoded using suitable feature descriptors [7].

Of the popular feature detectors, the Harris corner detector [9] is efficient at detecting local features, especially corners, on the soles of shoes [10]. The Harris corner detector relies on the image's autocorrelation function to detect points with strong intensity variations in a local neighbourhood. In other words, regions with a large positive corner response score correspond to corners, whereas regions with low values represent flat areas [11].

Theoretically, the shoe sole composition, tread pattern and degree of wear affect the sediment retention. Hence, this study aims to evaluate three types of shoe sole materials to examine the spatial dynamics of residues on the shoe sole and reveal the relative importance of different areas of the shoe sole. The image data were carefully analysed via image processing tools to elucidate the impact of shoe sole materials and BMI status. The study's insights can strengthen the evidentiary value of footwear impression evidence in criminal investigations and enhance its probative value in court.

Materials and Methods

Samples Preparation

Three subjects with varying BMI status, as outlined in Table 1, voluntarily participated in this study. All subjects provided written informed consent before participation. Each subject repeatedly stepped on the sandy substrate while wearing three different types of shoes (Table 2). Worn shoes, rather than new ones, were deployed as the former better represent what is likely to be encountered at a real crime scene.

To mimic a real crime scene, a rectangular paper tray (approximately, 70 cm × 210 cm) filled with sand was prepared. Each subject was instructed to relax before walking on the tray. After walking at least three steps, the subject carefully removed the shoe and recorded using a digital camera (Canon EOS 3000D with 18-55mm III Lens and DSLR). All images were captured using ISO 400 and f/15. A scale was placed next to the footwear outsoles before photography. Then, the shoe sole was carefully cleaned with a soft brush before the next sample was taken. Each subject was required to prepare three replicate samples for each of the three shoe types.

In total, a total of 54 impressions were prepared for this study (i.e., three volunteers × three shoes types × three stepping trials, × both left and right feet. For validation purposes, replicate data sampling was performed approximately two months apart, involving only Subjects 1 and 2. The same subjects were asked to repeat the process, but only the right foot was included. Hence, two data sets were prepared: Set A, comprising 54 images, and Set B, comprising 18 images. Figure 1 illustrates the composition of the two data sets.

Table 1: Biological backgrounds of three subjects participated in this work

ID	BMI Statuses	Foot Length (mm)
W1	Underweight	236
W2	Normal	225
W3	Overweight	243

Table 2: Details of the worn shoes studied in this work

ID	Shoe Type (Sole Materials)
S1	Men low-cut boot (rubber)
S2	Female slip-on sneaker (proprietary resin)
S3	Female clog (EVA foam-ethylene vinyl acetate)

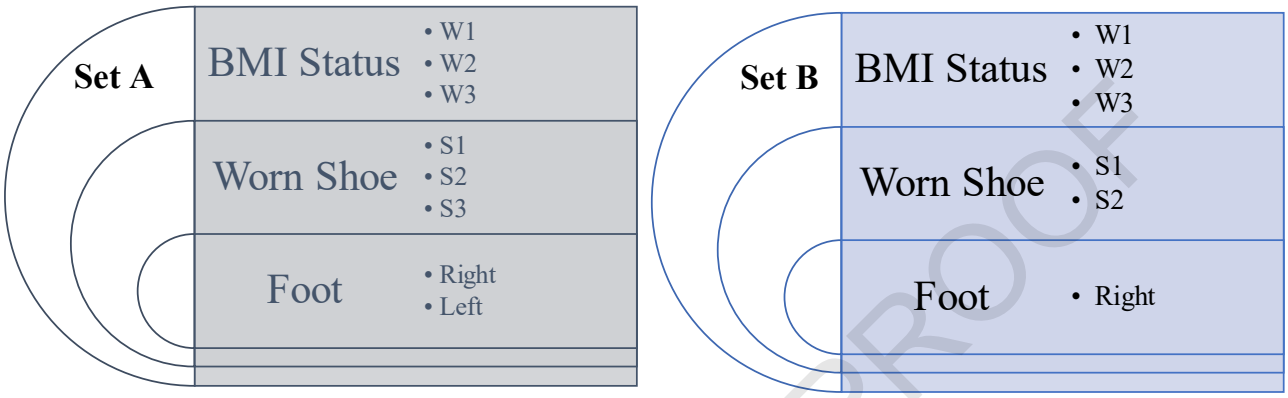

Figure 1: Compositions of dataset A and B, respectively consisting of three factors: (a) BMI status, (b) type of shoe sole materials, and (c) foot

Data Processing

The resulting images were all processed using R software (version 2.10.1). First, the raw digital images were carefully cropped to minimise blank regions. All images corresponding to the same shoe type were cropped into the same dimension: (a) S1 (2,700 × 1,200), (b) S2 (2,700 × 1,250), and (c) S3 (2,500 × 1,250). Subsequently, the cropped images were converted to grayscale. To ensure optimal results, the images were further pre-processed using min-max normalisation in the EBImage R package [12]. This step enhanced the clarity of the features on the shoe sole. Finally, the images were divided into equal-sized regions and processed using the Harris corner detector via the CornerDetectionHarris R package [13]. Figure 2 shows examples of images for S1, S2, and S3, divided into ten distinct sub-regions.

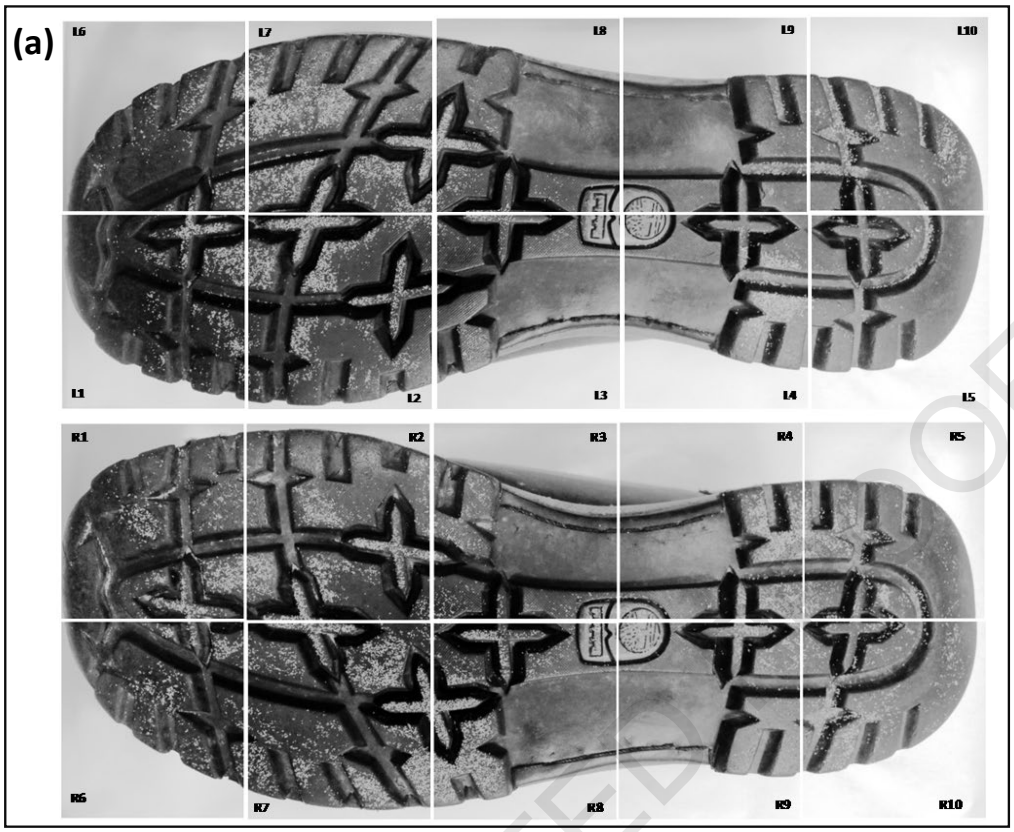

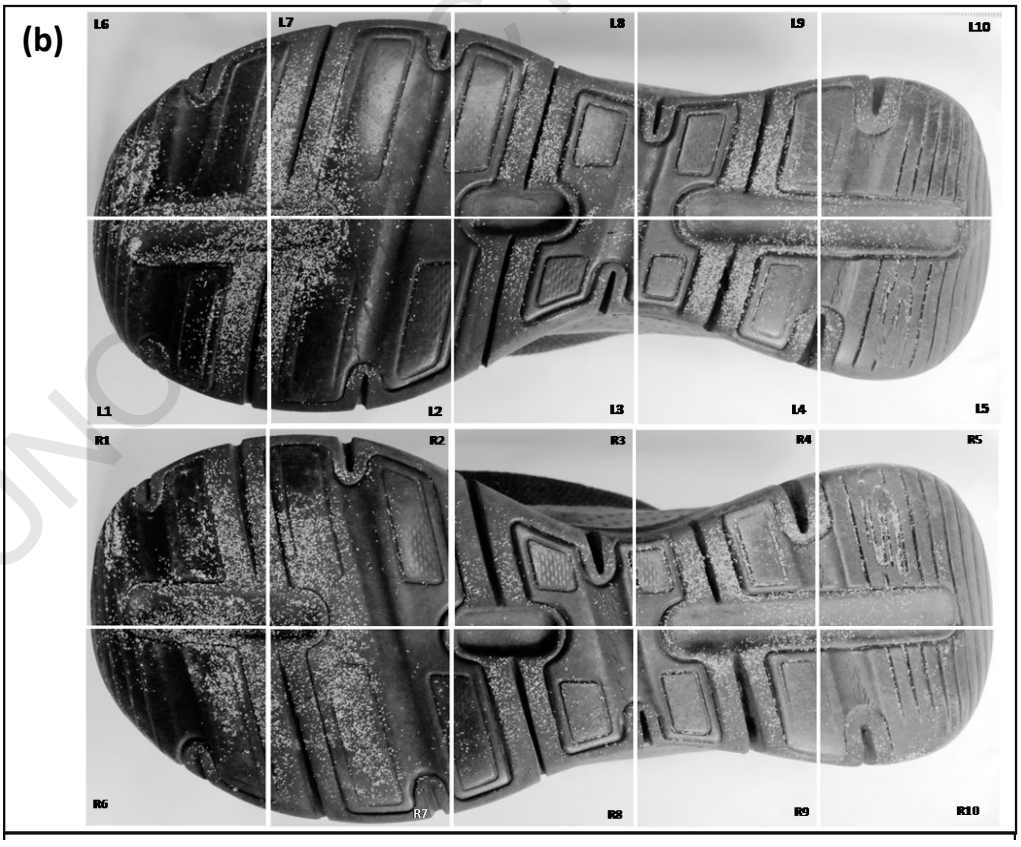

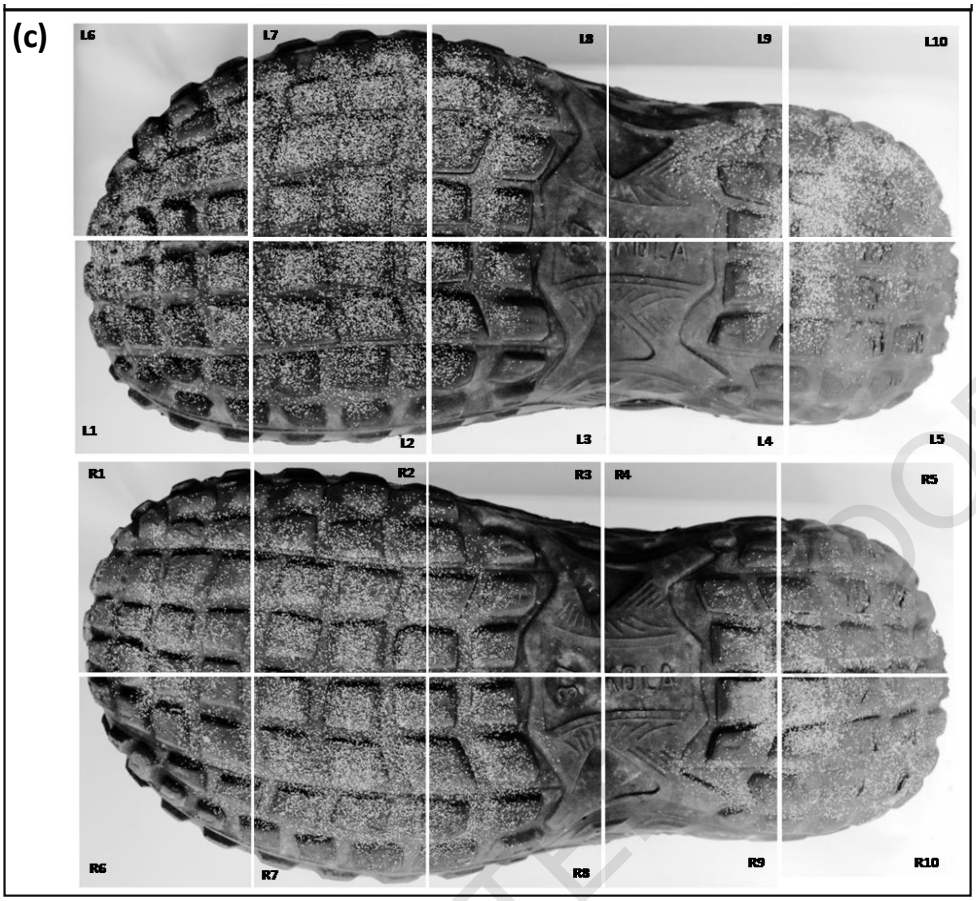

Figure 2: Shoe sole divided into ten exclusive sub-regions shown by shoe types: (a) S1, (b) S2, and (c) S3

Data Interpretation

To facilitate a visual examination of the distribution of sand particles on the shoe sole, the Harris corner algorithm was applied to estimate 10 quantitative values per image. As noted above, Harris corner is typically applied as a feature detector in a forensic footwear image retrieval system. Initially, central differences were used to estimate the image gradient by computing derivatives in the x and y directions for each pixel of an image. Then, the products of the gradients are estimated to compute the autocorrelation matrix. Finally, the Harris measure proposed by Harris and Stephens is applied to calculate the corner strength at each pixel in the image using Equation (1):

$$R_H = \lambda_1\lambda_2 - k \cdot (\lambda_1+\lambda_2)^2 = \det(M) - k \cdot trace(M)^2 \quad (1)$$

where k is a value ranging between 0.04 and 0.06, λ_1 and λ_2 are the eigenvalues of the autocorrelation matrix [11].

A positive R value denotes a corner, and a small R value represents a flat region. Herein, the strength value derived from the Harris corner detector was used as a quantitative measure of the amount of sand particles deposited on the shoe sole. For brevity, the strength value was summed across all pixels of a region. Consequently, each image of the shoe sole was represented by ten values. Dataset A was deployed to elucidate the impacts of shoe sole materials, BMI status, and foot (left or right) on retention capability and variability across the

ten sub-regions of a shoe sole. Meanwhile, dataset B was applied to illustrate the robustness of the study.

Results and Discussions

The effects of shoe sole materials and BMI status on the retention capability of the shoe sole were first evaluated for the left and right feet. Then, the retention capability of ten sub-regions on the shoe sole was discussed. All based on the dataset A. Finally, the robustness of the study, based on data collected over two months (dataset B) was presented.

Impact of Shoe Sole Materials, BMI Status and Foot (Left or Right) on Retention Capability

For brevity, total strength across the ten sub-regions was computed for the three wearers and shoe types to elucidate the impact of shoe sole materials on sand particle retention. Figure 3 illustrates bar charts showing the total strength values of Harris corner across three shoe types and wearers with different BMI status for the right and left feet. The results were based only on the data set A.

At first glance, the trends observed for the right foot were highly similar to those of the left foot. The lowest and highest strength values are consistently observed with S1 and S3, respectively, regardless of the wearer's BMI. Specifically, the highest total value was achieved by W2 while wearing S3. Meanwhile, W3 obtained the lowest total values by wearing S1. Which means, S3 demonstrated the highest capacity to retain sand particles; meanwhile, S1 retained comparatively fewer particles.

Regarding the BMI statuses, W2 and W3 had the lowest total values across the three shoe types for the left and right feet, respectively. On the contrary, the highest total values across the three shoe types were observed in the left foot of W1 and the right foot of W2. This means, W2 showed the greatest differences between the left and right feet based on the total values, i.e., the right foot exhibited a substantially higher soil retention capability than the left foot. Meanwhile, W1 and W3 demonstrated mild variation between the left and right foot based on the total values.

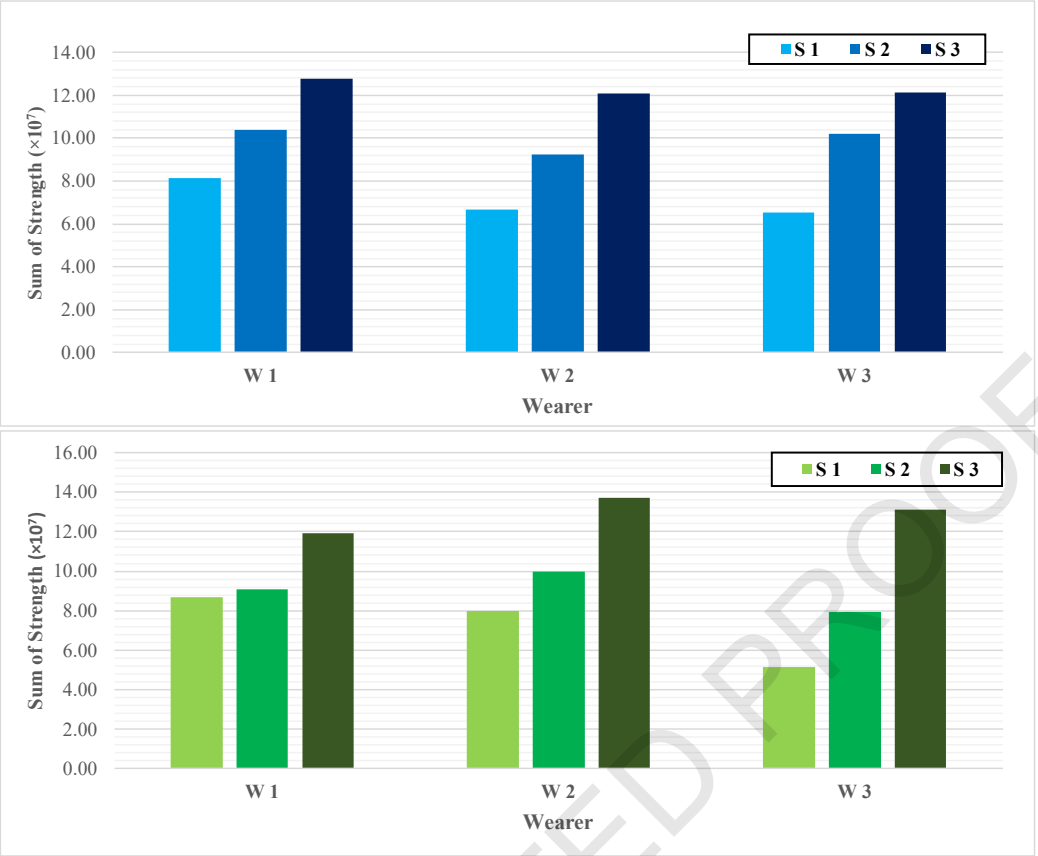

Figure 3: Bar charts showing sum of strength over the ten regions of a shoe sole by three wearers respectively represented by underweight (W1), normal (W2) and overweight (W3) BMI status; (top) left, and (bottom) right foot

Retention Capability of Shoe Sole Regions

Next, the differences between the ten sub-regions of the soles were examined for retention capability. For this purpose, the total strength values were presented for three wearers, ten sub-regions, three shoe types, and two feet, in Figure 4. Only dataset A was considered.

Overall, the quantity of sand particles retained varied across the ten sub-regions of the shoe sole. Nonetheless, S1 and S3 exhibited similar trends, regardless of foot and BMI status. For both shoe types, sub-regions 2 (i.e., L2 and R2) and 7 (i.e., L7 and R7) consistently had the highest total strength values. In particular, the highest values were observed in S3, which aligns with earlier findings that S3 showed the highest capacity to retain sand particles. On the contrary, the distribution patterns seen in the left and right feet of S2 were inconsistent with each other. Sub-regions 2, 3, and 4 of the right foot scored relatively higher than the same sub-regions of the corresponding sub-regions of the left foot, which exhibited substantially higher total strength values at sub-regions 7, 8, and 9.

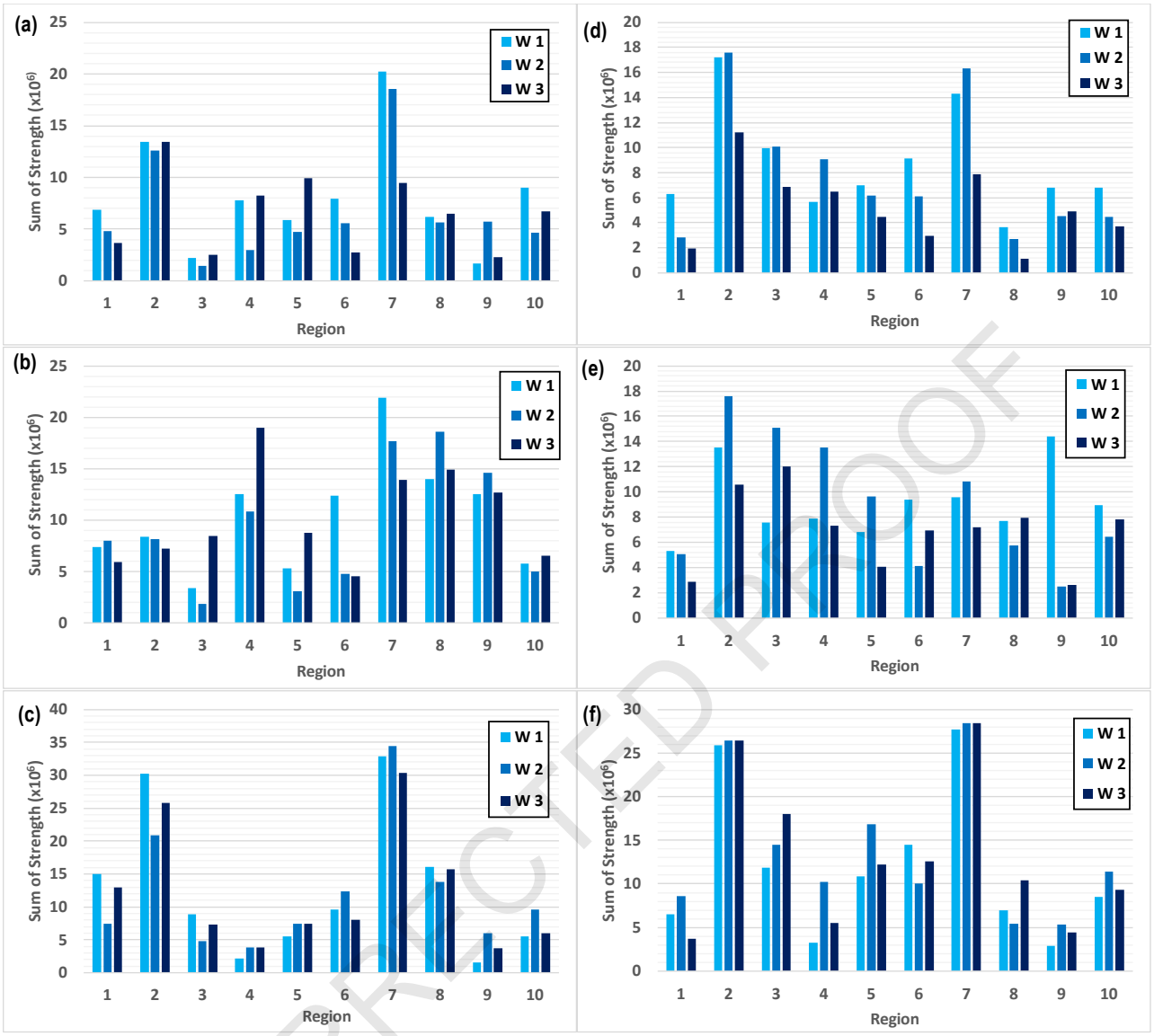

Figure 4: Bar charts showing total of strength values by the ten regions of a shoe sole according to shoe type: (a, d) S1, (b, e) S2, (c, f) S3; and foot: (a-c) left, (d-f) right

Among the sub-regions with relatively higher sums of strength values, only the sub-region L7 (i.e., left foot) of S1 and S2 showed a clear negative correlation with BMI status. In contrast, the negative correlation between BMI status and the total of strength value was only seen at the sub-region R2 (i.e., right foot) of S1. Meanwhile, the total of strength values for sub-region R3 (i.e., right foot) of S3 was positively associated with BMI status.

Robustness of the Study

To assess the robustness of the study, datasets A and B were compared by considering the right foot across three different BMI statuses (i.e., W1, W2, W3) and two shoe types (i.e., S1, S2). Figure 5 shows the bar charts of the total of strength values by the ten sub-regions. The robustness was assessed by comparing the relative differences in the total values derived from the same wearer and shoe type across two different sampling periods (i.e., sets A and B).

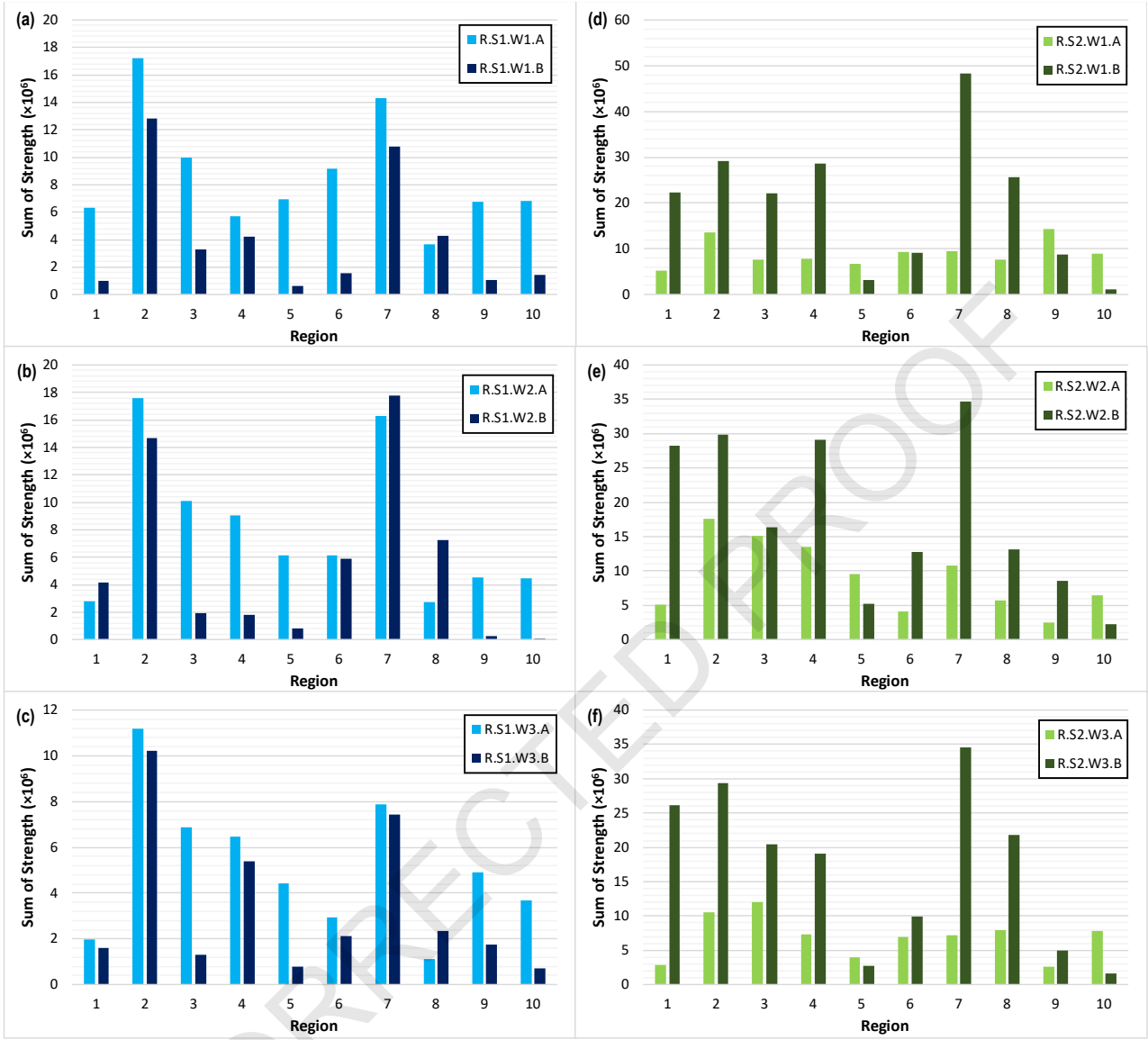

Figure 5: Bar charts showing the total of strength values by the ten regions of a right shoe sole according to shoe type: (a-c) S1, (d-f) S2; BMI status: (a, d) W1, (b, e) W2, and (c, f) W3. Light blue and green bars denote data set A; dark blue and dark green bars indicate data set B

Overall, the distribution of the total of strength values by the ten sub-regions across the two sampling periods was not 100% similar for S1 and S2. Nonetheless, sub-regions with a relatively higher total of strength values (i.e., better capability to retain sand particles) were consistent across the two sampling periods. Specifically, the highest total values were observed at sub-regions 2 and 7, regardless of wearers and time periods, for S1. On the other hand, sub-regions 1 to 4 of S2 tended to show a relatively higher total of strength values over the two sampling periods.

General Remarks

Insights into the spatial dynamics of trace evidence indicators (transfer and persistence) can contribute to improving practices in the examination of footwear impressions. The findings revealed the effects of shoe sole materials, BMI status, and foot and foot (left or right) on the spatial dynamics distribution and retention of sand particles underneath the shoe sole.

Retainability of sand particles, (i.e., adherence properties), was shown to be vary with shoe sole material. Theoretically, the adherence property (ability to bond with adhesives or other materials) Theoretically, adherence (the ability to bond with other materials) is influenced by surface characteristics and chemical composition [14]. The present study found that ethylene-vinyl acetate (EVA) exhibited the highest adherence. The adhesion of EVA is largely dependent on its vinyl acetate (VA) content. Higher VA content increases flexibility and viscosity, thereby enhancing bonding strength [15]. Consequently, the influence of BMI status was largely overshadowed by the high adherence of EVA.

In contrast, S1,[16] in particular, untreated styrene-butadiene rubber (SBR) and natural rubber (NR) exhibit poor inherent adhesion to polar materials due to the lack of polar functional groups. Which utilised a rubber-based sole, demonstrated the lowest adherence property. Rubber is generally hydrophobic and non-polar, thus often requires surface activation to achieve strong adhesion [16]. Rubber, especially untreated styrene-butadiene rubber (SBR) or natural rubber (NR), typically has poor inherent adherence to polar adhesives. Rubber surfaces are often hydrophobic (water-repellent) following a lack polar chemical groups.

In terms of physical properties, EVA is extremely lightweight, flexible, and provides effective cushioning and shock absorption [17], whereas rubber is denser than EVA. Proprietary resin-based shoe sole materials, often based on polyurethane (PU). Despite the obvious variation in weight, wearers of different BMI statuses tended to produce broadly similar retention patterns. This suggests that BMI status plays a limited role in influencing the adherence properties of sand particles compared to shoe sole material.

However, a relationship between BMI status and retainability was observed for S1, whereas it was least evident for S3. An inverse relationship between wearer weight and sand retention capabilities was identified.

Contrary to initial expectations, individuals with lesser weight will demonstrate a greater sand-retention on the shoe outsoles. This may be explained by differences in applied pressure, lighter persons exerted less downward force on the sandy substrate, while walking, resulting lower compaction and a looser arrangement of the sand grains. These loosely packed sand particles are more readily transpirable via electrostatic forces and capillary action when moisture is present.

In contrast, heavier individuals, exert greater pressure, inducing a greater dilatancy effect, allowing the moisture to penetrate deeper into the surrounding sand and away from the shoe shoe–surface interface [18]. This reduces the available moisture on the contact surface, which reduces adhesion via cohesive forces.

Sand grain particles adhere to shoe outsoles due to the influence of forces such as Van Der Waals interactions, electrostatic attraction, and small moisture bridges, which are stronger than the gravitational pull on a small scale [19]. For a smaller particle such as sand, the high surface area-to-mass ratio results in more effective attachment forces. Lighter individuals exert

less pressure, so more sand grains remain on the ground surfaces in a loose arrangement. Thus, the loose sand particles are available to be transferred to the shoe outsoles upon contact.

It is important to emphasise that this study introduces the Harris Corner detector as a as a quantitative proxy for estimating the number of sand particles retained on a shoe sole. To date, applying the corner strength values for this purpose has never been reported in the available literature. Theoretically, the Harris Corner relies on mathematical approaches for identifying points resembling corners or areas of high-intensity change in all directions [20]. Sand particles observed in this study exhibit sharp, angular edges rather than rounded shapes. Preliminary examinations suggest that the Harris corner strength is likely directly proportional to the number of sand particles adhering to the shoe sole surface (Figure 1). Accordingly, the summed corner strength values were used as an indicator of retained sand particles

Limitations of the Study

The findings of this study are subject to several limitations. First, each BMI category was represented by only one subject. Although, it was found that the influence of BMI was only more pronounced with the rubber-based soles. Future studies should consider increasing the number of subjects per BMI category to improve statistical robustness .

Second, only the sandy substrate was considered examined at a real forensic context, a variety of soil types may be encountered.

Finally, while this study demonstrates the feasibility of using the Harris corner detector to estimate retained particles, no formal validation was conducted to confirm the relationship between corner strength values and actual particle counts. Future work should include controlled validation experiments to quantify this relationship.

This research paper also demonstrated the feasibility of applying the Harris Corner detector at estimating the number of sand particles retained by a sole. No specific validation study was performed to assess the assumption proposed in this research paper. Therefore, future studies should include a well-designed test to estimate the correlation between the number of retained sand particles and the strength value of the Harris Corner detector.

Conclusions

In conclusion, ethylene vinyl acetate (EVA) shoe sole materials demonstrated the highest adherence property compared to polyurethane (PU) and rubber. Consequently, the influence of BMI cannot be readily deduced from an EVA shoe sole due to its extremely high adherence. Meanwhile, a rubber-based outsole is more likely to show a variation in particle retention with regard to BMI: Lighter individuals RW shown to retain more sand than heavier individuals, contradicting generally accepted assumptions and underscoring the importance of understanding the physics behind particle adhesion in forensic settings. To strengthen the validity and robustness of the findings, future investigations should encompass other substrate types (e.g., loam soils) and a wider range of shoe sole materials.

Additionally, the reliability of Harris Corner strength values as an indication of the quantity of retained particles on the shoe sole in a controlled setting must also be assessed. The results of this study are expected to contribute to the growing body of knowledge on forensic footwear analysis and lay the groundwork for the development of increasingly complex

analytical frameworks, in line with the dynamic nature of residue transfer and retention in real-world investigative situations.

Authors' Contributions

All authors contributed to the study conception and design. All authors read and approved the final manuscript. Conceptualisation: Loong Chuen Lee; Methodology: Li Yen Soo, Anwar AMA Salem, Faisal Ariffin @Othman; Formal analysis and investigation: Li Yen Soo, Loong Chuen Lee; Writing - original draft preparation: Li Yen Soo; Writing - review and editing: Loong Chuen Lee; Funding acquisition: Loong Chuen Lee; Resources: Loong Chuen Lee, Faisal Ariffin @ Othman; Validation and visualisation: Loong Chuen Lee; Supervision: Loong Chuen Lee.

Acknowledgements

This research was funded by the Faculty of Health Sciences, Universiti Kebangsaan Malaysia, Malaysia through the TAP grant (TAP-K016373).

Conflict of Interest Statement

The authors declare no conflict of interest. The funders had no role in the design of the study; in the collection, analyses, or interpretation of data; in the writing of the manuscript, or in the decision to publish the results.

References

[1] Bhuyan, M. K. (2019). Image descriptors and features. In *Computer vision and image processing* (pp. 150–205). CRC Press.

[2] Canny, J. (1986). A computational approach to edge detection. *IEEE Transactions on Pattern Analysis and Machine Intelligence*, *8*, 679–698. https://doi.org/10.1109/TPAMI.1986.4767851

[3] Cubbage, H., Macey, C., & Scott, K. (2023). Macroscopic assessment of environmental trace evidence dynamics in forensic settings. *Science & Justice*, *63*(3), 376–386. https://doi.org/10.1016/j.scijus.2023.03.004

[4] Ebnesajjad, S., & Landrock, A. H. (2015). Introduction and adhesion theories. In S. Ebnesajjad & A. H. Landrock (Eds.), *Adhesives technology handbook* (3rd ed., pp. 1–18).

[5] Fitzpatrick, R. W., & Donnelly, L. J. (2021). An introduction to forensic soil science and forensic geology: A synthesis. *Geological Society London Special Publications*, *492*(1), 1–32. https://doi.org/10.1144/sp492-2021-81

[6] Grant, B. F., Charles, J. P., D'Aout, K., Falkingham, P. L., & Bates, K. T. (2024). Human walking biomechanics on sand substrates of varying foot sinking depth. *Journal of Experimental Biology*, *227*, 1–14. https://doi.org/10.1242/jeb.246787

[7] Hao, Q., Yao, Z., Choi, W. J., & Kim, H. (2024). Effect of ethylene vinyl acetate foam-graphene composite material on the mechanical properties of sports footwear. *Alexandria Engineering Journal*, *96*, 142–148. https://doi.org/10.1016/j.aej.2024.04.006

[8] Jafarnezhadgero, A., Fatollahi, A., Amirzadeh, N., Siahkouhian, M., & Granacher, U. (2019). Ground reaction forces and muscle activity while walking on sand versus stable ground in individuals with pronated feet compared with healthy controls. *PLOS ONE*, *14*(9), Article e0223219. https://doi.org/10.1371/journal.pone.0223219

[9] Kapica, R., Tyczkowski, J., Balcerzak, J., Makowski, M., Sielski, J., & Worwa, E. (2019). Enhancing adhesive joints between commercial rubber (SBS) and polyurethane by low-pressure plasma surface modification. *International Journal of Adhesion and Adhesives*, *95*, Article 102415. https://doi.org/10.1016/j.ijadhadh.2019.102415

[10] Ménard, H., Cole, C., Gray, A., Mudie, R., Klu, J. K., & Daéid, N. N. (2021). Creation of a universal experimental protocol for the investigation of transfer and persistence of trace evidence: Part 1 — From design to implementation for particulate evidence. *Forensic Science International Synergy*, *3*, Article 100165. https://doi.org/10.1016/j.fsisyn.2021.100165

[11] Morgan, R. M., Freudiger-Bonzon, J., Nichols, K. H., Jellis, T., Dunkerley, S., Zelazowski, P., & Bull, P. A. (2009). The forensic analysis of sediments recovered from footwear. In K. Ritz, L. Dawson, & D. Miller (Eds.), *Criminal and environmental soil forensics* (pp. 253–269). Springer. https://doi.org/10.1007/978-1-4020-9204-6_16

[12] Morgan, R. M., Meakin, G. E., French, J. C., & Nakhaeizadeh, S. (2019). Crime reconstruction and the role of trace materials from crime scene to court. *Wiley Interdisciplinary Reviews: Forensic Science*, *2*(1), 1–18. https://doi.org/10.1002/wfs2.1364

[13] Moyano, M. A., Paris, R., & Martin-Martinez, J. M. (2019). Viscoelastic and adhesion properties of hot-melts made with blends of ethylene-co-n-butyl acrylate (EBA) and ethylene-co-vinyl acetate (EVA) copolymers. *International Journal of Adhesion and Adhesives*, *88*, 34–42. https://doi.org/10.1016/j.ijadhadh.2018.11.001

[14] Nibouche, O., Bouridane, A., Gueham, M., & Laadjel, M. (2009). Rotation invariant matching of partial shoeprints. *International Machine Vision and Image Processing Conference*, 94–98. https://doi.org/10.1109/IMVIP.2009.24

[15] Pau, G., Fuchs, F., Sklyar, O., Boutros, M., & Huber, W. (2010). EBImage — an R package for image processing with applications to cellular phenotypes. *Bioinformatics*, *26*(7), 979–981.

[16] Rida, I., Al-Maadeed, N., Al-Maadeed, S., & Bakshi, S. (2020). A comprehensive overview of feature representation for biometric recognition. *Multimedia Tools and Applications*, *79*, 4867–4890. https://doi.org/10.1007/s11042-018-6808-5

[17] Sanchez, J., Monzon, N., & Salgado, A. (2018). An analysis and implementation of the Harris corner detector. *Image Processing on Line*, *8*, 305–328. https://doi.org/10.5201/ipol.2018.229

[18] Stoney, D. A., Bowen, A. M., & Stoney, P. L. (2016). Loss and replacement of small particles on the contact surfaces of footwear during successive exposures. *Forensic Science International*, *269*, 78–88. https://doi.org/10.1016/j.forsciint.2016.11.015

[19] Wijffels, J., Perez, J. S., & Getreuer, P. (2025). *R package 'image.CornerDetectionHarris': Implementation of the Harris corner detection for images* (Version 0.1.2).

[20] Wu, Y., Dong, X., Shi, G., Zhang, X., & Chen, C. (2022). Crime scene shoeprint image retrieval: A review. *Electronics*, *11*(16), Article 2487. https://doi.org/10.3390/electronics11162487